4. H. Tagouchi, J. Konishi, N. Ishii, M. Yoshida, *J. Biol. Chem.* **266**, 22411 (1991).
5. H. R. Saibil *et al.*, *Curr. Biol.* **3**, 265 (1993).
6. T. Langer, G. Pfeifer, J. Martin, W. Baumeister, F.-U. Hartl, *EMBO J.* **11**, 4757 (1992).
7. L. A. Svensson, B. P. Surin, N. E. Dixon, M. D. Spangfort, *J. Mol. Biol.* **235**, 47 (1994).
8. G. N. Chandrasekhar, K. Tilly, C. Woolford, R. W. Hendrix, C. Georgopoulos, *J. Biol. Chem.* **261**, 12414 (1986).
9. P. V. Viitanen, A. A. Gatenby, G. H. Lorimer, *Protein Sci.* **1**, 363 (1992).
10. K. Braig, M. Simon, F. Furuya, J. F. Hainfeld, A. L. Horwich, *Proc. Natl. Acad. Sci. U.S.A.* **90**, 3978 (1993).
11. E. S. Bochkareva and A. S. Girshovich, *J. Biol. Chem.* **267**, 25672 (1992); J. Martin *et al.*, *Nature* **352**, 36 (1991); N. Ishii, H. Tagouchi, H. Sasabe, M. Yoshida, *J. Mol. Biol.* **236**, 691 (1994).
12. P. V. Viitanen *et al.*, *Biochemistry* **29**, 5665 (1990).
13. T. E. Gray and A. R. Fersht, *FEBS Lett.* **292**, 254 (1991).
14. G. S. Jackson *et al.*, *Biochemistry* **32**, 2554 (1993).
15. M. J. Todd, P. V. Viitanen, G. H. Lorimer, *ibid.*, p. 8560.
16. E. S. Bochkareva, N. M. Lissin, G. C. Flynn, J. E. Rothman, A. S. Girshovich, *J. Biol. Chem.* **267**, 6796 (1992).
17. M. J. Todd, P. V. Viitanen, G. H. Lorimer, *Science* **265**, 659 (1994).
18. M. Schmidt, M. J. Todd, G. H. Lorimer, P. V. Viitanen, *J. Biol. Chem.* **269**, 10304 (1994).
19. S. J. Landry, J. Zeilstra-Ryalls, O. Fayet, C. Georgopoulos, L. M. Gierasch, *Nature* **364**, 255 (1993).
20. J. Martin, M. Mayhew, T. Langer, F.-U. Hartl, *ibid.* **366**, 228 (1993).
21. M. Schmidt and J. Buchner, unpublished results.
22. In a previous attempt to investigate complex formation in the presence of ATP, the complex was formed in the presence of ATP and subsequently applied to a size-exclusion column with ATP in the running buffer (*5*). However, this treatment changes the equilibrium of free compared with bound GroES, because released GroES is immediately removed on the column. This change in equilibrium might be why only asymmetric complexes were detected in electron micrographs.
23. A. Azem and P. Goloubinoff, *Science* **265**, 653 (1994).
24. J. Frank, A. Verschoor, M. Boublik, *ibid.* **214**, 1353 (1981).
25. M. Van Heel and J. Frank, *Ultramicroscopy* **6**, 187 (1981). All computations were performed with either the SEMPER [W. O. Saxton, T. J. Pitt, M. Horne, *ibid.* **9**, 109 (1979)] or EM (R. Hegerl and A. Altbauer, *ibid.*, p. 109) software systems.
26. An important preparative detail would be the time of incubation of the two proteins in the presence of ATP, before the sample is applied to the grid, because the ADP-ATP ratio is continuously changing. We routinely waited 30 min before preparing the samples for electron microscopy. Under the conditions used, we were sure that an excess of ATP was still present.
27. In a later report the observed stoichiometry of two GroES rings associated with one GroEL oligomer has been questioned by the authors [N. Ishii, H. Tagouchi, M. Sumi, M. Yoshida, *FEBS Lett.* **299**, 169 (1992)].
28. To be sure that no damage of the oligomeric proteins due to freezing procedures was occurring, we rapidly purified the protein without freezing it between individual purification steps (Fig. 1). However, when the so purified proteins were frozen and then again allowed to form complexes in the presence of ATP, we observed no differences on negatively stained electron micrographs. Thus, freezing did not change the structural and functional properties of GroE particles.
29. O. Fayet, J.-M. Louarn, C. P. Georgopoulos, *Mol. Gen. Genet.* **202**, 435 (1986).
30. J. Buchner *et al.*, *Biochemistry* **30**, 1586 (1991).
31. We thank W. Baumeister for equipment for image analysis and discussions, S. Volker-Mürkl for technical assistance, and the University of Regensburg, the Deutsche Forschungsgemeinschaft, and the Fonds der Chemischen Industrie for financial support to M.S., R.R., R.J., and J.B.

5 April 1994; accepted 27 June 1994

Dynamics of the Chaperonin ATPase Cycle: Implications for Facilitated Protein Folding

Matthew J. Todd, Paul V. Viitanen, George H. Lorimer*

The *Escherichia coli* chaperonins GroEL and GroES facilitate protein folding in an adenosine triphosphate (ATP)–dependent manner. After a single cycle of ATP hydrolysis by the adenosine triphosphatase (ATPase) activity of GroEL, the bi-toroidal GroEL formed a stable asymmetric ternary complex with GroES and nucleotide (bulletlike structures). With each subsequent turnover, ATP was hydrolyzed by one ring of GroEL in a quantized manner, completely releasing the adenosine diphosphate and GroES that were tightly bound to the other ring as a result of the previous turnover. The catalytic cycle involved formation of a symmetric complex (football-like structures) as an intermediate that accumulated before the rate-determining hydrolytic step. After one to two cycles, most of the substrate protein dissociated still in a nonnative state, which is consistent with intermolecular transfer of the substrate protein between toroids of high and low affinity. A unifying model for chaperonin-facilitated protein folding based on successive rounds of binding and release, and partitioning between committed and kinetically trapped intermediates, is proposed.

Chaperonins are ubiquitous, indispensable proteins that facilitate protein folding in an ATP-dependent manner (*1*), enhancing the yield (but rarely the rate of formation) of properly folded substrate protein under conditions where spontaneous folding does not occur (*2*). Chaperonins are typified by the two *E. coli* heat shock proteins GroEL (chaperonin 60) and GroES (chaperonin 10) (*1*). GroEL forms a binary complex with many unfolded proteins (*3*) and thus is promiscuous rather than selective. To achieve the native state under nonpermissive conditions, a substrate protein must be discharged from the binary complex in a state that allows commitment to the native state, which usually requires the complete chaperonin system of GroEL, GroES, and the hydrolysis of ATP (*4*). Here, we describe how these three components interact with each other to assist protein folding. We propose that, in contrast to other models, the unfolded protein substrate plays a passive role in this process.

GroEL (*5*) consists of two stacked heptameric rings of seven identical 57-kD subunits each (*6*). GroES is a single homoheptameric toroid of 10-kD subunits (*7*). GroEL has a K^+-dependent adenosine triphosphatase (ATPase) activity (one turnover every 10 to 12 s) that is inhibited by GroES (*6–12*). The binding of one ring of GroES to one of the two rings of GroEL, which occurs only in the presence of adenine nucleotide, creates an asymmetric complex of $GroES_7 \cdot ADP_7 \cdot GroEL_7$–$GroEL_7$ (where ADP is adenosine diphosphate) (*5, 9*). The stoichiometry of this species has been inferred from kinetic measurements of GroEL ATPase activity (*8–12*) and observed directly by electron microscopy (*13, 14*). GroES binding inhibits GroEL ATPase from 50 to 100%, depending on the concentrations of ATP, ADP, and K^+ (*9*). At high K^+ concentrations, half of the sites remain fully active, resulting in 50% inhibition. At low K^+ concentrations, the ATPase activity of GroEL can be completely inhibited by a single ring of GroES after as little as one-half of the GroEL protomers (seven sites) have turned over (*9*). This complete inhibition can be reversed by raising the concentration of either ATP or K^+ or by removing the inhibitory ADP. Under such circumstances, ATP hydrolysis resumes at ~50% of the uninhibited rate. The GroES inhibition reflects a decreased affinity of unoccupied sites of the asymmetric complex for ATP (relative to ADP) (*9*).

Steady-state kinetics, however, do not provide an adequate description of the chaperonin ATPase cycle. We therefore exploited the slow hydrolysis of ATP and the stability of the asymmetric complex to analyze the dynamics of the chaperonin system. To examine the consequences of a single round of ATP hydrolysis (all seven sites on one ring of GroEL turning over once), we manipulated the concentrations of K^+, ATP, and ADP to turn on or off the hydrolysis of ATP at will, while the integrity of the chaperonin proteins was maintained.

E. I. DuPont de Nemours and Company, Central Research and Development Department, Experimental Station, Wilmington, DE 19880, USA.

*To whom correspondence should be addressed.

In the absence of GroES, ATP hydrolysis by GroEL proceeded in a linear manner, without a burst or a lag before the appearance of inorganic phosphate (P_i) (Fig. 1A) (*9*, *15*); thus, steps preceding or following ATP hydrolysis (that is, substrate binding and product dissociation) were not rate-determining (cycle I of Fig. 2). The reaction could be inhibited by >85% by adding a 10-fold excess of the competing nucleotide ADP (Fig. 1A), or it could be completely inhibited by removing Mg^{2+} with EDTA (*16*). In both cases, the onset of inhibition was essentially instantaneous, because the data points obtained after the quench extrapolated back to the data point obtained at the time of the quench (arrow in Fig. 1A). Thus, ATP within the active site of GroEL at the time of the quench is not committed to hydrolysis, but instead dissociates.

Similar experiments were done in the presence of GroES (Fig. 1B) with the use of low concentrations of K^+ to form and preserve the completely inhibited asymmetric chaperonin complex (species B of Fig. 2) (*9*). This complex formed after half of the GroEL ATP-binding sites (the seven sites on one GroEL toroid) had turned over once (*9*), thus synchronizing all of the molecules in the same inhibited state (Fig. 1B). Inhibition was relieved by raising the concentrations of K^+ and of [γ-^{32}P]ATP (maintaining the same specific activity), which initiated cycle II (Fig. 2) (arrow 1 in Fig. 1B) (*17*) and allowed the resumption of ATP hydrolysis. Shortly thereafter, we switched the system off by imposing one of three nondenaturing quenches (arrow 2 in Fig. 1B): chelation of free Mg^{2+} with EDTA, addition of ADP, or addition of unlabeled ATP to dilute the specific activity of the [γ-^{32}P]ATP 20 times. In contrast to the situation in the absence of GroES, none of these three conditions resulted in an immediate cessation of [γ-^{32}P]ATP hydrolysis. Instead, [γ-^{32}P]ATP hydrolysis corresponding to about one-half of the site (7 mol of ATP hydrolyzed per mole of GroEL) continued before inhibition took hold. Thus, upon reactivation one of the two heptameric rings became completely committed to ATP hydrolysis. When ADP was added before the concentrations of K^+ and [γ-^{32}P]ATP were increased, the system remained uncommitted and the original inhibited state persisted (Fig. 1B, open circles). This order-of-addition effect also showed the effectiveness of the nondenaturing ADP quench. Likewise, if the initial inhibition was relieved by the addition of K^+ and unlabeled ATP, no burst of [γ-^{32}P]ATP hydrolysis was observed, indicating that the remaining sites on the complex did not contain [γ-^{32}P]ATP that was committed to hydrolysis before the addition of K^+ and [γ-^{32}P]ATP. These results were independent of the GroES concentration beyond that required to make the asymmetric complex, even with a 10-fold excess of GroES to GroEL.

The above result suggested that in the presence of GroES the hydrolysis of ATP by GroEL became quantized. We tested this idea by forming the fully inhibited asymmetric complex at a low concentration of K^+, re-initiating ATP hydrolysis by raising the K^+ and [γ-^{32}P]ATP concentrations, then at various times within the next 30 s arresting hydrolysis with $HClO_4$ or one of two nondenaturing quenches, either excess ADP or unlabeled ATP. Thirty seconds after the nondenaturing quench, $HClO_4$

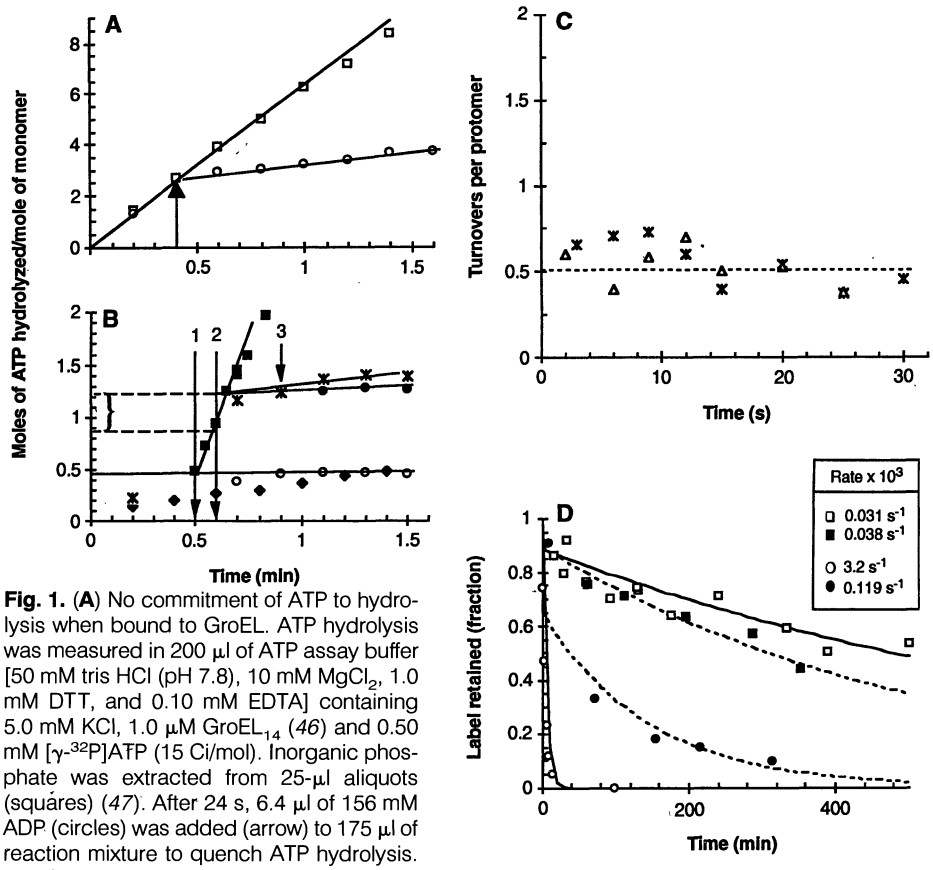

Fig. 1. (**A**) No commitment of ATP to hydrolysis when bound to GroEL. ATP hydrolysis was measured in 200 μl of ATP assay buffer [50 mM tris HCl (pH 7.8), 10 mM $MgCl_2$, 1.0 mM DTT, and 0.10 mM EDTA] containing 5.0 mM KCl, 1.0 μM $GroEL_{14}$ (*46*) and 0.50 mM [γ-^{32}P]ATP (15 Ci/mol). Inorganic phosphate was extracted from 25-μl aliquots (squares) (*47*). After 24 s, 6.4 μl of 156 mM ADP (circles) was added (arrow) to 175 μl of reaction mixture to quench ATP hydrolysis. (**B**) Commitment of ATP to hydrolysis when bound to the asymmetric complex. Asymmetric complexes of $GroES_7$·ADP_7·$GroEL_7$–$GroEL_7$ were generated by adding 20 μl of 1.0 mM [γ-^{32}P]ATP (15 Ci/mol) and 5.0 mM KCl to 180-μl reactions containing 1.0 μM GroEL (14-mer) and 1.43 μM GroES (7-mer) in ATP assay buffer (diamonds). At 30 s (arrow 1), ATPase activity of the asymmetric complex was reactivated by a second addition of [γ-^{32}P]ATP (7.0 μl of 10 mM ATP, also at 15 Ci/mol, and 100 mM K^+) to the remaining 175 μl of each reaction (squares). At 35 to 36 s (arrow 2), nondenaturing quenches [5.6 μl of 156 mM ADP (solid circles) or 17.5 μl of 50 mM ATP (asterisks)] were added to 175 μl of the reaction mixture, and ATP hydrolysis was measured for a further 60 s. If ADP was added before the second addition of ATP (open circles), the initial inhibition was not relieved, demonstrating the effectiveness of the ADP quench. (**C**) Quantized hydrolysis by half of the sites of the asymmetric complex after a nondenaturing quench. Inhibited complexes of $GroES_7$·ADP_7·$GroEL_7$–$GroEL_7$ were created by adding 5.0 μl of 5.0 mM KCl and 1.0 mM [γ-^{32}P]ATP (73 Ci/mol) to 40 μl of 1.25× ATP assay buffer containing 1.25 μM $GroEL_{14}$ and 2.5 μM $GroES_7$. After 30 s, the complex was reactivated by adding 5.0 μl of 50 mM KCl and 10 mM [γ-^{32}P]ATP (73 Ci/mol) [arrow 1 in (B)]. Further [γ-^{32}P]ATP hydrolysis was either quenched at the indicated times by addition of $HClO_4$ or 5.0 mM ADP (triangles) or the specific activity of the ATP was diluted 10 times (asterisks) [arrow 2 in (B)]. Reactions subjected to a nondenaturing ADP or ATP quench were treated with $HClO_4$ 30 s later [arrow 3 in (B)]. The quantity of [γ-^{32}P]ATP hydrolyzed after the nondenaturing quench was determined by subtracting the quantity of [^{32}P]P_i at the time of the nondenaturing quench [arrow 3 minus arrow 2 in (B)]. (**D**) Spontaneous dissociation of the asymmetric complex. Isolated $GroES_7$·[α-^{32}P]ADP_7·$GroEL_7$–$GroEL_7$ complex was incubated at 25°C with 0 (open squares) or 1.0 (closed squares) mM ADP or at 0°C with 0 (open circles) or 1.0 (closed circles) mM ADP. Free nucleotide was separated from the complex with gel filtration. Lines were drawn by fitting the data to a first-order decay, giving the rate constants for loss of bound [α-^{32}P]ADP (inset). The dissociation rate depended on both the concentration of the complex (320 nM $GroES_7$·[α-^{32}P]ADP_7·$GroEL_7$–$GroEL_7$) and the buffer composition. If the concentration of Mg^{2+} was raised to 10 mM, the rate of dissociation decreased ~33% to 0.020 × 10^{-3} s^{-1}; if the Mg^{2+} concentration was lowered to 2 mM, the rate increased fourfold.

was added. Regardless of when the nondenaturing quenches were imposed, an average of 0.56 ± 0.14 or 0.53 ± 0.11 mol of $[^{32}P]P_i$ per mole of GroEL were released after the ADP or ATP quench, respectively (Fig. 1C). Thus, one of the two heptameric GroEL rings was committed to ATP hydrolysis. In contrast to the behavior of GroEL alone, GroES induced the active sites of GroEL to display complete cooperativity, functioning as discrete heptameric units.

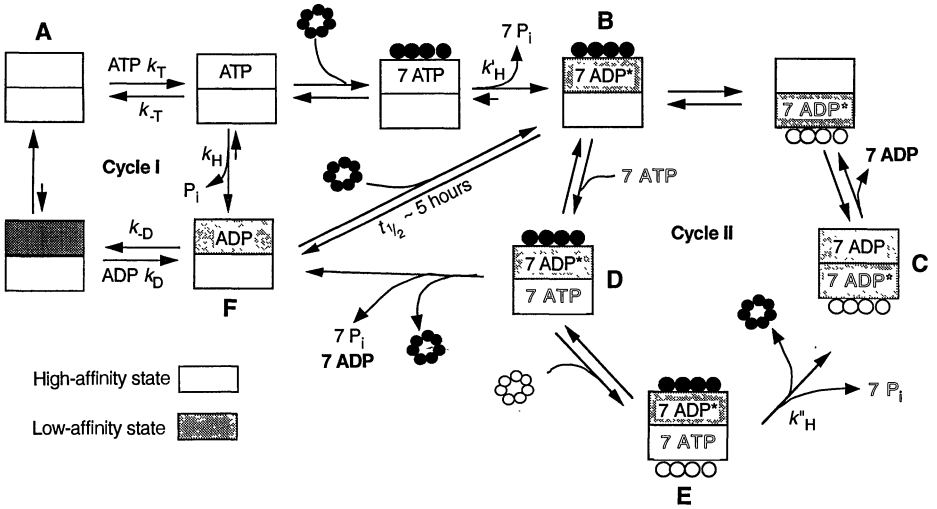

Fig. 2. Scheme for the hydrolysis of ATP by GroEL in the absence (cycle I) and presence (cycle II) of GroES. ATP hydrolysis by GroEL alone involves two heptameric rings, represented here as stacked "bricks" (species A), a schematic version of the side views seen in the electron microscope (*6, 13, 14, 25*). For simplicity, ATP hydrolysis is shown occurring in only one of the two rings. Upon addition of ATP or ADP and one ring of GroES (shown in black), a stable asymmetric complex (species B) is formed containing seven tightly bound ADP molecules (asterisk). Images of these particles appear as bullet-shaped objects in side view (*13, 14, 24, 25*). Addition of ATP to species B initiates cycle II and creates species D, which is committed to hydrolysis. Addition of a second ring of GroES (shown in white) creates the structurally symmetric species E, which appears as football-shaped particles in side view (*25*). Species E is not completely populated because it is an intermediate in cycle II. Hydrolysis of ATP by species E releases the black GroES ring, and the tightly bound ADP in species B is now free to dissociate; the other toroid now contains the tightly bound ligands. As a result of the high-affinity to low-affinity (H to L) transition that accompanies ATP hydrolysis, unfolded substrate protein is given an opportunity to dissociate when that ring is converted to the L state. At present, we cannot formally exclude the possibility that ATP hydrolysis by species D proceeds before a second ring of GroES binds, returning the system to cycle I (species F). The rate constants k_T, k_{-T}, k_D, and k_{-D} describe the association and dissociation of ATP and ADP, respectively, from GroEL alone. The rate constants k_H, k'_H, and k''_H describe the rate-determining hydrolysis of ATP.

Table 1. Dissociation of the $GroES_7$·$[\alpha\text{-}^{32}P]ADP_7$·$GroEL_7$–$GroEL_7$ complex (*45, 50*). AMP-PNP, adenylylimidodiphosphate (Boehringer Mannheim).

Additions	Time	$[\alpha\text{-}^{32}P]$ADP retained (%)
	Controls	
1. None	5 hours	65
2. 1 mM ADP	5 hours	60
3. 10 mM KCl	5 hours	62
4. 1 mM ADP and 10 mM KCl	5 hours	39
5. 1 mM ADP, 10 mM KCl, and 3.7 μM GroES	5 hours	37
6. 0.01% Tween-20	1 hour	73*
	ATP and ATP analogs	
7. 500 μM ATP and 5 mM KCl	15 s	<5
8. 2 mM ATP-γ-S and 5 mM KCl	1 min	96
9. 2 mM AMP-PNP and 5 mM KCl	1 min	84
	Single turnover conditions	
10. 500 μM ATP and 5 mM KCl; after 15 s, add 2 mM ADP	1 min	<5
11. 2 mM ADP; after 15 s, add 500 μM ATP and 10 mM KCl	1 min	95
	Metal ion requirement	
12. 10 mM EDTA	<1 min	<1

*The $GroES_7$·ADP_7·$GroEL_7$–$GroEL_7$ complex will slowly dissociate spontaneously (Fig. 3). The reported loss of label under the indicated condition is expressed as a percentage of the amount of label that would be retained if no additions had been made.

Before determining the fate of the ligands bound to the asymmetric chaperonin complex under single turnover conditions, we assessed its stability. The complex was formed with a slight molar excess of GroES to GroEL in the presence of low concentrations of K^+ and $[\alpha\text{-}^{32}P]$ATP. After removal of unbound ligands (GroES and nucleotide) by gel filtration, the isolated complex contained 6.5 ± 1.6 mol of $[\alpha\text{-}^{32}P]$ADP or 1 mol of $[^{35}S]GroES_7$ per mole of $GroES_7$·ADP_7·$GroEL_7$–$GroEL_7$ (*5*). The $[\alpha\text{-}^{32}P]$ADP slowly dissociated from this complex with first-order kinetics [half-time ($t_{1/2}$) ~5 hours] (Fig. 1D). A 500-fold molar excess of unlabeled ADP, increased K^+ concentration, increased GroES concentration, or combinations of these did not increase the loss of $[\alpha\text{-}^{32}P]$ADP more than two times (Table 1, entries 1 through 5). Because the complex was stable to the conditions of the nondenaturing ADP quench, the consequences of a single turnover could be explored.

When we restarted ATP hydrolysis by the isolated complex by raising the concentrations of K^+ and ATP (Fig. 1B) and the complex was immediately reisolated, none of the original $[\alpha\text{-}^{32}P]$ADP remained bound (Table 1, entry 7). This result was not observed with ATP analogs (Table 1, entries 8 and 9) at concentrations where they inhibit ATPase activity (*11, 18*). Thus, the binding of ATP to the unliganded ring of GroEL is not sufficient to cause dissociation of the ADP that is tightly bound to the other GroEL ring in the complex. To determine if a single round of ATP hydrolysis on one GroEL toroid suffices to release the $[\alpha\text{-}^{32}P]$ADP, we exploited the nondenaturing ADP quench. Under "single turnover" conditions, complete exchange of tightly bound $[\alpha\text{-}^{32}P]$ADP was observed (Table 1, entry 10). As before, order of addition experiments confirmed the efficacy of the ADP quench (Table 1, entry 11).

Unexpectedly, lowering the temperature to 0°C caused the complex to dissociate ~100 times faster ($t_{1/2}$ = 3.6 min); this effect was diminished to one-fifteenth its previous level by an excess of unlabeled ADP (Fig. 1D) (*19*). Therefore, the binding of ADP to the unliganded ring of the asymmetric complex (Fig. 2, species C) enhanced its stability. A second unexpected condition—removal of Mg^{2+} by EDTA at 25°C—also caused rapid complex dissociation (Table 1, entry 12), which is consistent with an additional function for Mg^{2+} in stabilizing the asymmetric complex beyond its association with the nucleotide (*20*).

Similar isotope exchange experiments were done with [^{35}S]GroES. Net loss of GroES by spontaneous dissociation of the complex was slow, with only ~25% lost after 190 min (Table 2), which parallels the rate of loss of tightly bound ADP (Fig. 1D). Bound [^{35}S]GroES was not in rapid equilibrium with unlabeled GroES in solution (Table 2, entry 3), even in the presence of excess ADP (Table 2, entry 4). This was consistent with the ligands being released in the reverse order to that in which they were bound (that is, ADP departs rapidly after the dissociation of GroES). As with bound ADP, the complex rapidly dissociated upon addition of EDTA (*16*) or if the temperature was lowered. At 0°C, excess ADP stabilized the complex, as indicated by the enhanced retention of both [α-^{32}P]ADP (Fig. 1D) and [^{35}S]GroES (Table 2). Unlabeled GroES reduced the specific activity of [^{35}S]GroES in the complex slightly (Table 2), demonstrating a slow equilibration of free and bound forms of GroES at low temperatures (compare Fig. 1D).

When the ATPase activity of the chaperonin complex was reactivated, bound [^{35}S]GroES rapidly exchanged with free, unlabeled GroES (Table 2, entry 5). As before, a single round of ATP hydrolysis sufficed to bring the bound GroES into isotopic equilibrium with the total GroES (Table 2, entry 6). Thus, we conclude that a single round of ATP hydrolysis on the GroEL toroid lacking bound GroES is both necessary and sufficient for the rapid discharge of both the ADP and the GroES from the opposite toroid.

A working hypothesis for the hydrolysis of ATP by GroEL in the presence and absence of GroES is presented in Fig. 2. As others have done (*8, 15, 21*), we invoke the existence of two alternating conformational states of the heptameric GroEL ring, with high (H) and low (L) affinity for nonnative substrate protein. The binding of nucleotide to the H and L states may induce other conformational changes (as observed by electron microscopy) (*13, 14, 22*), which are necessary for GroES binding. We further propose that ATP hydrolysis drives the H to L transition.

In the absence of GroES, the catalytic cycle of ATP hydrolysis by *E. coli* GroEL (cycle I of Fig. 2) is relatively simple. In the absence of nucleotide (the resting state), the equilibrium strongly favors the H state (species A of Fig. 2). The interactions of GroEL with ATP and K^+ are cooperative and synergistic (*8–12, 15*). Because no "burst" of P_i production is apparent at the onset of the reaction (Fig. 1A) (*9, 15*), we conclude that ADP dissociation (k_{-D}) and the L to H transition are not rate-determining ($k_{-D} > k_H$, where k_H = rate of ATP hydrolysis). Furthermore, nondenaturing quench experiments (Fig. 1A) revealed that little of the ATP bound at the active site at the time of the quench was committed to hydrolysis (that is, the dissociation of ATP, where $k_{-T} > k_H$).

In the presence of GroES, the cycle of ATP hydrolysis (cycle II of Fig. 2) is more complex. GroEL and GroES do not interact in the absence of nucleotide (*7, 9, 10*). Thus, the formation of the asymmetric complex involves the ordered addition of ligands: nucleotide binding precedes GroES binding to one of the two heptameric toroids of GroEL. Evidence consistent with the nucleotide and GroES being bound to the same toroid of GroEL in the asymmetric complex has been reported (*23*). At low K^+ concentrations (1 mM), the complex can be formed after only one of the two toroids hydrolyzed ATP, yielding tightly bound ADP within the asymmetric complex (species B, Fig. 2). The rate of ATP hydrolysis in forming the asymmetric complex (k'_H) is the same as the rate of ATP hydrolysis by GroEL alone (9) ($k_H = k_H$) (Fig. 2). The asymmetric complex can also be made with ADP (9); however, in this case higher concentrations of nucleotide or longer times are required (*9, 13*). Cycle II may then be said to begin with the asymmetric complex (species B of Fig. 2).

The remaining seven active sites in the asymmetric complex can still be occupied by nucleotide. If that nucleotide is ADP (as in species C of Fig. 2), hydrolysis is prevented. Thus, we envision the fully inhibited asymmetric complex to be an equilibrium between species B and species C, with the equilibrium being dependent on the concentration of free ADP. At low K^+ concentrations, complete inhibition occurs with virtually no occupancy of the remaining free sites by ADP (9). If that nucleotide is ATP (species D, Fig. 2), however, a cycle of hydrolysis at seven of the sites is set in motion that cannot be arrested until complete. The commitment of all seven sites of the asymmetric complex to ATP hydrolysis suggests that the function of GroES is to coordinate the hydrolysis of ATP on a GroEL toroid in a quantized or highly cooperative manner. For this reason, both ADP and ATP quenches are followed by the release of 7 mol of [^{32}P]P_i per mole of GroEL (Fig. 1C). If all seven sites have to be occupied by ATP, then occupying any one site with ADP would represent a particularly effective means of inhibition.

Once ATP hydrolysis is initiated, the system must pass through several intermediate states before the cycle is completed (Fig. 2); this results in complete release of the tightly bound ligands ADP and GroES with each round of ATP hydrolysis. This model accounts for why, during steady-state ATP hydrolysis in the presence of GroES, the ATP hydrolysis rate is reduced by 50% when compared with that of GroEL alone. In cycle II, half of the sites are occupied by ADP at all times and thus are unable to hydrolyze ATP.

Symmetrical, football-shaped (*24*) particles (species E of Fig. 2) can be observed in the electron microscope and can be inferred to exist by cross-linking studies (*25*). These structures can be observed only when more GroES is present than GroEL and when MgATP or nonhydrolyzable analogs are present (*26*). If the chaperonin complexes are formed with ADP, or if all ATP is consumed, only asymmetrical bullet-shaped particles are observed (Fig. 2, species B and C) (*25*). Our model does not require that this symmetrical species be stoichiometrically populated because in cycling between species D to E to C to B (Fig. 2), GroES functions catalytically. The fact that "footballs" accumulate in the presence of excess

Table 2. Dissociation of the [^{35}S]$GroES_7$·ADP_7·$GroEL_7$–$GroEL_7$ complex (*45, 51, 52*). Theoretical isotopic equilibrium was reached when the amount of ^{35}S retained decreased to 9%.

Additions	Time (min)	Temperature (°C)	[^{35}S]GroES retained (%)
	Controls		
1. None	25	25	94
2. None	190	25	75
3. 4.3 μM GroES	90	25	79
4. 4.3 μM GroES and 2 mM ADP	90	25	80
	Single turnover conditions		
5. 4.3 μM GroES, 1 mM ATP, and 5 mM KCl	<1	25	12
6. 4.3 μM GroES, 1 mM ATP, and 5 mM KCl; after 15 s, add 5 mM ADP	<1	25	16
	Low-temperature dissociation		
7. None	60	0	10
8. 2 mM ADP	60	0	72
9. 2 mM ADP and 4.3 μM GroES	60	0	58

GroES suggests that they precede a slow step in the catalytic cycle. As in cycle I, the slow step of cycle II is the hydrolysis of ATP ($k_H = k''_H$, where k''_H is the rate of ATP hydrolysis by football-shaped complexes).

Although the football-shaped particles appear structurally symmetrical, the functionally symmetrical species $GroES_7 \cdot ADP_7 \cdot GroEL_7$–$GroEL_7 \cdot ADP_7 \cdot GroES_7$ can be ruled out for three reasons. First, no symmetrical particles are observed by electron microscopy or by cross-linking when GroEL, GroES, and ADP are combined (*25*). Second, the existence of a symmetric species, however transient, would provide a mechanism for exchange of [α-^{32}P]ADP and [^{35}S]GroES from the chaperonin complex, which does not occur. Finally, if ATP hydrolysis produced a functionally symmetrical complex, each round of ATP hydrolysis would release only half of the tightly bound ligands ADP and GroES. Because each round of hydrolysis brings about the complete discharge of these ligands, the complex must be functionally asymmetrical, perhaps by having ADP bound to the one GroEL toroid and ATP bound to the other toroid (species E). This model also accounts for two apparently conflicting observations. Antibody to an unfolded protein had been observed to bind GroEL on the toroid opposite GroES (*26*) (species B, Fig. 2). In contrast, cross-linking studies suggest that unfolded protein and GroES are bound to the same toroid, at least transiently (*27*) (species E, Fig. 2).

It has been asserted that unfolded proteins specifically induce the dissociation of the asymmetric complex (*23*), leading to a model in which the unfolded substrate protein plays an active role in the chaperonin reaction cycle. Attempts to replicate these experiments led to the observation that low concentrations of guanidine HCl, carried over with these unfolded proteins, could account for the reported destabilization of the asymmetric chaperonin complex (*16*). Urea or acid-denatured proteins did not release the tightly bound [^{32}P]ADP (*16*). Physiological dissociation occurs as a result of ATP hydrolysis; thus, the unfolded protein apparently exploits the chaperonin cycle rather than controlling it.

Current models for chaperonin-assisted protein folding are based on observations that the nonnative proteins bind within the central cavity of GroEL (*14, 28*). Variants of this model (*23, 29*) incorporate the idea that the unfolded protein substrate oscillates intramolecularly between the two GroEL toroids as successive rounds of ATP hydrolysis drive the two toroids between alternating states of high and low affinity for nonnative protein. The protein is finally discharged from the lumen in a state that is committed to proceeding to the native state. By allowing protein folding to occur within the cavity (that is, at infinite dilution), this mechanism circumvents second-order aggregation problems. Examination of GroEL by electron microscopy, however, indicates that there may be no passage between the two toroids (*22*). In addition, the singly toroidal chaperonin 60s of the mammalian mitochondria and *Thermoanaerobacter brockii* together with chaperonin 10 assist protein folding (*30*). With these chaperonins, intramolecular transfer would require the transient formation of double-ringed structures, for which there is currently no evidence.

A test of the current model would be to determine what happens to a radiolabeled substrate protein, initially bound to GroEL, after a single round of ATP hydrolysis in the presence of a molar excess of free, unlabeled substrate protein. The model predicts that the substrate protein would remain sequestered through multiple rounds of ATP hydrolysis, emerging only when it has reached a conformation that is no longer recognized by GroEL (that is, a state committed to the native state). Accordingly, no isotopic dilution of the GroEL–substrate protein complex should occur after a single round of ATP hydrolysis. On the other hand, if the substrate protein was transferred intermolecularly before attaining a committed state, a substantial isotopic dilution of the GroEL–substrate protein complex would occur after each cycle of ATP hydrolysis. This test requires a pool of relatively long-lived, unlabeled, nonnative substrate protein to exchange with the GroEL-bound, radiolabeled substrate protein. Because the nonnative states of most proteins tend to rapidly partition to aggregates or to the native state [conformations that are no

Table 3. Dissociation of the chaperonin·[^{35}S]RuBisCO-I complexes. Final concentrations (*45*) were 50 nM RuBisCO-I, 0.5 mM ADP or ATP, and 114 nM $GroES_7$ (*53–55*). Theoretical isotopic equilibrium occurred when counts per minute decreased to ~5 to 10% (*56*). ND, none detected at all indicated time points.

Additions	[^{35}S]RuBisCO eluting with GroEL (%) after time (min)				Native RuBisCO (%)
	1	20	60	120	
Additions to isolated GroEL–[^{35}S]RuBisCO-1					
1. None		100*		85	ND
2. RuBisCO-I	89		70	77	ND
3. ATP	57		34		ND
4. RuBisCO-I and ATP	49		15		ND
5. RuBisCO-I and ADP	81		66		ND
6. ATP and GroES	46				ND
			16		61
7. ATP, GroES, and RuBisCO-I	44				ND
		19			37
			13		37
Additions to isolated $GroES_7 \cdot ADP_7 \cdot GroEL_7$–$GroEL_7$[^{35}S]RuBisCO-I					
8. None		100*		86	ND
9. RuBisCO-I	96		74		ND
10. RuBisCO-I and ADP	61		27		ND
11. RuBisCO-I and ATP	37				<5
			11		47

*Immediate re-injection of the GroEL-bound RuBisCO onto the gel-filtration column is designated as 100%. The actual amount varied from 75 to 80% of the total disintegrations per minute re-injected. We expect the remainder adhered to various surfaces involved. Values presented are accurate to within ±5%.

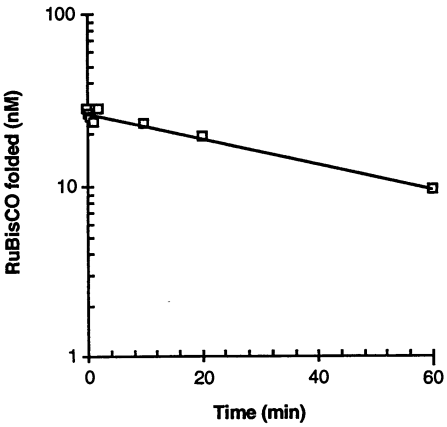

Fig. 3. Stability of RuBisCO-I in chloride-free buffer. We rapidly added 5 μl of 2.0 μM acid-denatured *Rhodosprillum rubrum* RuBisCO in 10 mM HCl (*48*) to 195 μl of folding buffer [100 mM Na Hepes (pH 7.8), 5 mM $Mg(CH_3CO_2)_2$, 0.5 mM KCH_3CO_2, 5 mM DTT, 0.1 mM EDTA, and 0.02% Tween-20 at 25°C]. At the indicated times, 10 μl of 1.2 μM $GroEL_{14}$ was added (57 nM after dilution), trapping any of the original 50 nM RuBisCO that had not aggregated. After 1 hour, reactions were adjusted to 5 mM KCH_3CO_2, 10 mM $Mg(CH_3CO_2)_2$, 1 mM ATP, and 94 nM $GroES_7$ to release and fold the bound RuBisCO. RuBisCO activity was assayed as described (*4*) after 20 min of folding ($t_{1/2}$ for the folding reaction under these conditions is ~2.5 to 3 min) (*49*).

longer recognized by GroEL (4)], we first sought conditions to enhance the lifetime of an unfolded substrate protein.

Under the conditions described in Fig. 3, conformers of RuBisCO (31) are formed (RuBisCO-I) that are kinetically trapped, as they do not progress to the native state (4). These conformers do not readily aggregate, as demonstrated by their failure to scatter light (16). A large fraction was able to be rescued by the chaperonin system for at least 60 min (Fig. 3). The conditions used to suppress aggregation had no apparent effect on the stability of the chaperonin complex (Table 1, entry 6). Thus, by setting the concentration of the chaperonin–[^{35}S]RuBisCO-I complex low enough (≤5 nM), a transient pool of unlabeled RuBisCO-I could be made available for isotopic exchange experiments.

Complexes of [^{35}S]RuBisCO-I, formed with either GroEL alone or with the asymmetric chaperonin complex, were isolated on a column capable of resolving these species from large aggregates and smaller components such as native RuBisCO (32). The isolated complexes containing [^{35}S]RuBisCO-I were tested with various combinations of nucleotide, unlabeled RuBisCO-I, and GroES and reisolated after 1 or 60 min. In the absence of unlabeled RuBisCO-I, [^{35}S]RuBisCO-I bound to either GroEL or the asymmetric complex tightly, with a net loss of only ~15% of the initially bound RuBisCO-I after 2 hours (Table 3, entries 1 and 8). As the conditions were not permissive for RuBisCO folding, none of the missing [^{35}S]RuBisCO appeared as native (32). When unlabeled RuBisCO-I was included as an exchange ligand, the loss of [^{35}S]RuBisCO-I from either complex was increased (Table 3, entries 2 and 9). Therefore, the [^{35}S]RuBisCO-I that dissociated in the absence of unlabeled, unbound RuBisCO-I was free to rebind to GroEL. Thus, the observed tight binding of unfolded proteins to GroEL represents a dynamic situation where bound protein equilibrates slowly with that free in solution, even in the absence of adenine nucleotides. The estimated value for $t_{1/2}$ for the dissociation of RuBisCO-I bound to GroEL was about 120 min. Assuming that the association rate between GroEL and the unfolded protein is diffusion-limited (~10^8 M^{-1} s^{-1}) (33), the overall dissociation constant computes to ~1 pM.

Although ADP had little effect on the dissociation of radiolabeled protein from GroEL, ATP increased the rate of release of RuBisCO-I more than 100-fold (Table 3, entries 2 and 4 to 7). With excess unlabeled RuBisCO-I and ATP, ~50% of the bound [^{35}S]RuBisCO-I was lost within the first minute, rapidly establishing isotopic equilibrium (Table 3, entries 3 and 4). But in the absence of GroES, none of the released [^{35}S]RuBisCO folded to the native state, even after 60 min (Table 3, entries 1 to 5). In contrast, when GroES and ATP were both present, [^{35}S]RuBisCO-I was lost from GroEL at a similarly rapid rate, but much of the released protein folded (Table 3, entry 6). Although the [^{35}S]RuBisCO-I was rapidly released from GroEL, it was not initially released in a committed state. Otherwise, much of the ^{35}S radioactivity would have eluted as the native protein. Instead, a maturation period or several cycles of release and binding are required for RuBisCO to achieve a native state (Table 3, entry 6). Because $t_{1/2}$ for chaperonin-assisted RuBisCO folding under these conditions is 3 ± 1 min, the rate-limiting step was not the release from GroEL. If ATP and GroES were added simultaneously with an excess of unlabeled RuBisCO-I, less native [^{35}S]RuBisCO was formed (Table 3, entry 7), which suggests that the RuBisCO released from GroEL (even in the presence of GroES) after a single round of dissociation was susceptible to aggregation. This result confirmed that the protein released from the chaperonin was not committed to becoming native.

Similar experiments were done with the isolated, quaternary complex GroEL·ADP·GroES·[^{35}S]RuBisCO-I. ATP caused rapid loss of [^{35}S]RuBisCO from the quaternary complex ($t_{1/2}$ ~0.7 min) (Table 3, entry 11), but again, the protein released within the first minute was not native. Complete isotopic equilibration was not achieved within the first minute, as additional loss of [^{35}S]RuBisCO-I occurred in the next 60 min. However, this conclusion rests on the assumption that all of the free, unlabeled RuBisCO-I was immediately available for ligand exchange, an assumption that may not be entirely correct (34). ADP significantly increased the exchange of [^{35}S]RuBisCO-I from the quaternary complex even though it had only a marginal effect on the exchange from GroEL (Table 3, compare entries 5 and 10). However, none of the released [^{35}S]protein progressed to the native state. Thus, single turnover experiments using a nondenaturing ADP quench to arrest ATP hydrolysis could not be done. Preliminary experiments quenching chaperonin-folding reactions with EDTA support the conclusion that multiple cycles of release and rebinding are necessary for RuBisCO folding. Our data are therefore inconsistent with the current model because most (>60%) of the bound protein was released in a nonnative state into free solution after one or a few rounds of ATP hydrolysis (Table 3, entries 7 and 11). Instead, our data suggest that after each turnover, the unfolded substrate protein is transferred intermolecularly.

Since the classic experiments of Anfinsen and others, we have known that an unfolded polypeptide possesses the information (encoded in the primary sequence) to fold to the native state (35). Yet, even when the pitfall of aggregation is avoided, some proteins do not revert to the native state (Fig. 3) (36). Moreover, the yield of properly folded protein is frequently so low (>5%) that an explanation is needed. The in vitro refolding of several small proteins involves multiple pathways with rapid kinetic partitioning to native and misfolded states (37). In these cases, the barrier separating the unfolded from the kinetically trapped states is small enough that it can be surmounted and the native state eventually reached. However, for many other proteins this kinetic barrier may be insurmountable (36). The yield of properly folded protein would then be defined by a partitioning factor ϕ (Fig. 4). These misfolded states may undergo further higher order aggregation reactions in vitro or form inclusion bodies in vivo. Alternatively, binding of these misfolded species to GroEL suppresses aggregation (38). Such a nonspecific function accounts for GroEL's known promiscuity (3). We agree with the proposal that GroEL uses binding energy to convert the substrate protein to a less folded state (15, 39). This suggestion is supported by recent

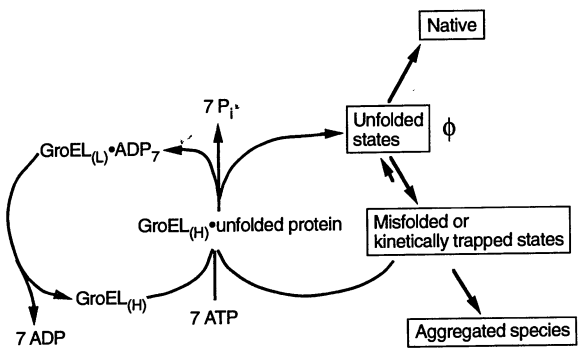

Fig. 4. The role of the chaperonin ATPase cycle in facilitated protein folding. Unfolded protein partitions to either the native state or an ensemble of misfolded states. The partition factor ϕ is equal to a ratio of native protein over the total of native and misfolded protein. Upon quantized hydrolysis of ATP by chaperonin complex, the unfolded protein is released to once again partition between native and misfolded states. Successive rounds of binding, ATP hydrolysis, release, and repartitioning ultimately result in the accumulation of the native state. Different proteins are characterized by different values for ϕ. For smaller, single-domain proteins ϕ tends toward unity, whereas for larger, multidomain proteins ϕ may be quite small, necessitating many rounds of ATP hydrolysis to reach the native state.

nuclear magnetic resonance evidence (*40*) showing the destabilization of the complete structure of a globular protein while bound to GroEL. We suggest that the thermodynamic barrier (*41*) separating GroEL-bound and free forms of the unfolded substrate protein is overcome by the hydrolysis of ATP in a quantized manner. All seven subunits in one GroEL toroid are converted from the high-affinity, low-energy H state to a low-affinity, high-energy L state, giving the nonnative protein an opportunity to dissociate (Fig. 4). The role of GroES is to coordinate the quantized interconversion of GroEL subunits. Thus, with each round of ATP hydrolysis unfolded protein can be released to the medium where, once again, it undergoes kinetic partitioning to native and misfolded states. Those molecules that misfold are repeatedly recycled through the chaperonin system undergoing successive rounds of intermolecular transfer, until eventually all of the substrate protein is converted to the native state.

REFERENCES AND NOTES

1. R. J. Ellis, R. A. Laskey, G. H. Lorimer, Eds., *Molecular Chaperones* (Chapman and Hall, London, 1993); J. Zielstra-Ryalls *et al.*, *Annu. Rev. Microbiol.* **45**, 301 (1991); C. Georgopoulos and W. J. Welch, *Annu. Rev. Cell Biol.* **9**, 601 (1993).
2. The terms "permissive" and "nonpermissive" are borrowed from bacterial genetics where they are used to describe conditions for growth. Here, we apply them to the conditions for the spontaneous folding of a protein. The distinction between permissive and nonpermissive conditions for spontaneous folding is rather arbitrary, however. Even under supposedly nonpermissive conditions, some small degree of spontaneous folding can usually be detected.
3. P. V. Viitanen, A. A. Gatenby, G. H. Lorimer, *Protein Sci.* **1**, 363 (1992); A. L. Horwich *et al.*, *Cell* **74**, 909 (1993).
4. P. Goloubinoff, J. T. Christeller, A. A. Gatenby, G. H. Lorimer, *Nature* **342**, 884 (1989); M. Schmidt *et al.*, *J. Biol. Chem.* **269**, 10304 (1994).
5. We refer to the doubly toroidal $GroEL_{14}$ (or $GroEL_7$–$GroEL_7$) as GroEL and to the singly toroidal $GroES_7$ as GroES. When specific interactions with individual toroids are implied, we revert to the more defined nomenclature. A long dash distinguishes the two heptameric GroEL rings to which the various ligands bind. For example, $GroES_7$·ADP_7·$GroEL_7$–$GroEL_7$ corresponds to the asymmetric complex in which one heptameric ring of GroES and seven ADP molecules are bound to the same ring of GroEL (*23*).
6. R. W. Hendrix, *J. Mol. Biol.* **129**, 375 (1979); T. Hohn *et al.*, *ibid.*, p. 359; V. L. Tsuprun *et al.*, *Biochim. Biophys. Acta* **1099**, 67 (1992).
7. G. N. Chandrasekhar *et al.*, *J. Biol. Chem.* **261**, 12414 (1986).
8. T. Gray and A. R. Fersht, *FEBS Lett.* **292**, 254 (1991).
9. M. J. Todd, P. V. Viitanen, G. H. Lorimer, *Biochemistry* **32**, 8560 (1993).
10. P. V. Viitanen *et al.*, *ibid.* **29**, 5665 (1990).
11. I. G. Badcoe *et al.*, *ibid.* **30**, 9195 (1991).
12. E. S. Bochkareva *et al.*, *J. Biol. Chem.* **267**, 6796 (1992).
13. T. Langer *et al.*, *EMBO J.* **11**, 4757 (1992).
14. H. Saibil *et al.*, *Nature* **353**, 25 (1991).
15. G. S. Jackson *et al.*, *Biochemistry* **32**, 2554 (1993).
16. M. J. Todd, P. V. Viitanen, G. H. Lorimer, unpublished results.
17. The resumption of activity occurred without a discernible lag or burst. This behavior is in contrast to the situation at the very outset of the experiment, when a burst was observed in the presence of GroES, during which time the activity declined from the uninhibited to the ~50% inhibited state and the asymmetric complex was formed (*9*).
18. F. Baynex and A. A. Gatenby, *J. Biol. Chem.* **267**, 11637 (1992).
19. The rapid dissociation of the asymmetric complex at 0°C may compromise the interpretation of proteolytic digestions conducted at low temperatures. The reported (*13, 23*) protection from proteolysis of one of the two GroEL toroids by GroES at 0°C is at best transient. Because the complex falls apart on ice, proteolysis goes cleanly to completion (*16*). The value for $t_{1/2}$ for this process corresponds approximately to the length of time used in the reported experiments (*16*)—hence the claim that half of the toroids are protected.
20. Data consistent with this hypothesis are also found in Fig. 1, where we note that the rate of spontaneous dissociation of the complex was dependent on the free Mg^{2+} concentration, and with the results of recent glutardialdehyde cross-linking experiments [A. Azem, S. Diamant, P. Goloubinoff, *Biochemistry* **33**, 6671 (1994)].
21. A. Horovitz, E. S. Bochkareva, O. Kovalenko, A. S. Girshovich, *J. Mol. Biol.* **231**, 58 (1993); T. Mizobata *et al.*, *J. Biol. Chem.* **267**, 17773 (1992).
22. H. R. Saibil *et al.*, *Curr. Biol.* **3**, 265 (1993).
23. J. Martin *et al.*, *Nature* **366**, 228 (1993).
24. We refer here to American football, not soccer.
25. M. Schmidt *et al.*, *Science* **265**, 656 (1994); A. Azem, M. Kessel, P. Goloubinoff, *ibid.*, p. 653; O. Llorca *et al.*, *FEBS Lett.* **345**, 181 (1994).
26. N. Ishii *et al.*, *J. Mol. Biol.* **236**, 691 (1994).
27. E. S. Bochkareva and A. S. Girshovich, *J. Biol. Chem.* **267**, 25672 (1992).
28. H. Saibil and S. Wood, *Curr. Opin. Struct. Biol.* **3**, 207 (1993); K. Braig *et al.*, *Proc. Natl. Acad. Sci. U.S.A.* **90**, 3978 (1993).
29. T. E. Creighton, *Nature* **352**, 17 (1991); D. A. Agard, *Science* **260**, 1903 (1993); R. J. Ellis, *Nature* **366**, 213 (1993).
30. P. V. Viitanen *et al.*, *J. Biol. Chem.* **267**, 695 (1992); K. J. Truscott, P. B. Høj, R. K. Scopes, *Eur. J. Biochem.* **222**, 277 (1994).
31. RuBisCO stands for ribulose 1,5-bisphosphate carboxylase-oxygenase.
32. Other forms of nonnative RuBisCO are retained on the column and can be eluted only with a denaturant.
33. T. Gray and A. R. Fersht, *J. Mol. Biol.* **232**, 1197 (1993).
34. The species generically referred to as RuBisCO-I (*42*) is likely a mixture of nonnative monomeric and oligomeric conformers in equilibrium with one another. Preliminary dynamic light scattering studies (*16*) indicate that some of this material is oligomeric. In the [^{35}S]ligand-exchange experiments, complete isotopic equilibration is calculated assuming that all of the free, unlabeled RuBisCO-I is monomeric and immediately available for exchange. To the extent that some of the free, unlabeled RuBisCO-I is not in a form that permits it to react with free GroEL, the maximum possible isotopic dilution is decreased. The yield of RuBisCO-I bound to GroEL reflects several experimental difficulties, including (i) the rapid aggregation of ~30% of the RuBisCO upon removal of the denaturing conditions (Fig. 3); (ii) the loss of RuBisCO at dilute concentrations to various surfaces involved; and (iii) the fact that although the [^{35}S]RuBisCO was isotopically pure, chemical purity of this carrier-free preparation was only ~50%, as judged by SDS–polyacrylamide gel electrophoresis (PAGE).
35. C. B. Anfinsen, *Science* **181**, 223 (1973).
36. D. Baker and D. A. Agard, *Biochemistry* **33**, 7505 (1994); W. Teschner, R. Rudolph, J. R. Garel, *ibid.* **26**, 2791 (1987); M. J. Bennett, S. Choe, D. Eisenberg, *Proc. Natl. Acad. Sci. U.S.A.* **91**, 3127 (1994); V. Schultes and R. Jaenicke, *FEBS Lett.* **290**, 235 (1991).
37. T. R. Sosnick *et al.*, *Nature Struct. Biol.* **1**, 149 (1994); T. A. Creighton, *ibid.*, p. 135; S. E. Radford *et al.*, *Nature* **358**, 302 (1992); G. A. Elove and H. Roder, *Am. Chem. Soc. Symp. Ser.* **470**, 50 (1991).
38. J. Buchner *et al.*, *Biochemistry* **30**, 1586 (1991).
39. R. A. Staniforth *et al.*, *Biochem. J.* **300**, 651 (1994); T. J. P. Hubbard and C. Sander, *Protein Eng.* **4**, 711 (1991).
40. R. Zahn *et al.*, *Nature* **368**, 261 (1994).
41. In the case of RuBisCO, the thermodynamic barrier between the free and GroEL-bound forms of the unfolded state corresponds to 16.4 kcal/mol.
42. S. M. van der Vies *et al.*, *Biochemistry* **31**, 3635 (1992).
43. P. Goloubinoff, A. A. Gatenby, G. H. Lorimer, *Nature* **337**, 44 (1989).
44. J. Pierce and S. Gutteridge, *Appl. Environ. Microbiol.* **49**, 1094 (1986); J. V. Schloss *et al.*, *Methods Enzymol.* **90**, 522 (1982); C. R. Somerville and S. C. Somerville, *Mol. Gen. Genet.* **193**, 214 (1984).
45. In Tables 1 to 3, additions refer to the final concentration of the added component, after more concentrated stock solution was added (≤5% volume change). Time refers to the time between the first addition of the indicated components (or initial complex isolation, when no additions were made) until injection onto the column.
46. The chaperonin proteins were purified from *E. coli* containing the plasmid pGroESL (*43*) and purified as described (*9*). Protein concentration was determined by quantitative amino acid analysis.
47. Inorganic phosphate (P_i) was determined by molybdo-phosphate extraction (*9*). All assays were performed at 25°C unless otherwise noted; to correct for background disintegrations per minute (0.5 ± 0.05%), complete time courses were run under all conditions in the absence of GroEL.
48. With use of acid-denatured substrate proteins, there are no "carry-over" effects, such as those that occur with guanidine hydrochloride. The use of guanidine hydrochloride–denatured RuBisCO was avoided because even low concentrations of guanidine hydrochloride not only promote aggregation of RuBisCO folding intermediates but also destabilize the asymmetric chaperonin complex (*16*).
49. Recombinant dimeric RuBisCO was purified from *E. coli* containing the plasmid pRR2119 encoding the RuBisCO gene from *Rhodosprillum rubrum* as described (*44*); we quantitated both by using the published extinction coefficient ($\varepsilon_{280\ nm}$ = 67,200 M^{-1} cm^{-1} (*44*) and by assaying for activity. RuBisCO concentrations throughout refer to subunit concentrations.
50. The $GroES_7$·[α-^{32}P]ADP_7·$GroEL_7$–$GroEL_7$ complex was formed by adding 3.2 μM $GroEL_{14}$ to 5.7 μM $GroES_7$ in 50 mM tris HCl (pH 7.8), 5 mM $MgCl_2$, 1.0 mM dithiothreitol (DTT), 0.10 mM EDTA, 0.50 mM KCl, and 100 μM [α-^{32}P]ATP (25 Ci/mol). After 1 min, 100 μl of complex was isolated from unbound nucleotide and excess $GroES_7$ by gel filtration (Sephacryl S-300; 1.5 cm by 10.5 cm; Pharmacia) in the same buffer lacking nucleotide, giving ~1 ml, with 6.5 ± 1 mol of ADP bound per mole of complex (now ~320 nM $GroES_7$·[α-^{32}P]ADP_7·$GroEL_7$–$GroEL_7$). The isolated complex was challenged with the indicated treatments, then re-injected onto the same column after the indicated interval in Table 1.
51. [^{35}S]GroES was purified from *E. coli* DS410 minicells containing the expression plasmid pGroESL (*43*) after 2 hours of labeling with 200 μCi of [^{35}S]methionine (1100 Ci/mmol; New England Nuclear). Washed minicells were disrupted with lysozyme [0.1 mg/ml in 10 mM EDTA, phenylmethylsulfonyl fluoride (0.1 μg/μl; Sigma), 0.01% Tween-20 (Bio-Rad), and 20 mM tris (pH 7.8)] and three freeze-thaw cycles, then spun at 17,500*g* for 20 min. The crude extract was desalted with a G-25 gel-filtration column (Pharmacia) equilibrated with 20 mM tris HCl, (pH 7.8), 0.1 mM EDTA, and 1 mM DTT, then applied to a Mono-Q HR 5/5 column (Pharmacia) (developed with 0 to 1 M NaCl in the same buffer) for anion-exchange chromatography. Fractions containing [^{35}S]GroES were identified by autoradiography after SDS-PAGE, pooled, concentrated, diluted into 50 mM succinate (pH 4.6), 0.1

mM EDTA, and 1 mM DTT, and applied to a Mono-S HR 10/10 column (developed with 0 to 1 M NaCl in the same buffer) for cation-exchange chromatography. GroES-containing fractions were identified by autoradiography as above. Following this second ion-exchange step, GroES was demonstrated to be isotopically pure by SDS-PAGE, and the concentration (54 Ci/mol) was determined by quantitative amino acid analysis.

52. Formation of the [^{35}S]GroES$_7$·ADP$_7$·GroEL$_7$–GroEL$_7$ complex was achieved by incubation of 4.3 μM GroEL$_{14}$ and 3.1 μM [^{35}S]GroES$_7$ (*45*) with 100 μM ATP for 5 min. The first round of gel-filtration chromatography (Bio-Sil Sec 400-5; 7.8 mm by 300 mm; Bio-Rad; 1 ml/min) diluted the complex ~10 times to ~430 nM. Aliquots of this complex were treated as indicated and reinjected onto the same column. The buffer throughout was 50 mM tris HCl, 10 mM $MgCl_2$, 0.50 mM DTT, 0.5 mM KCl, and 50 μM EDTA (pH 7.8).
53. [^{35}S]RuBisCO was generated as described (*44*) diluting the specific activity with unlabeled RuBisCO. The ion-exchange chromatography step was modified by developing the Mono-Q HR 5/5 column with a 0.01 to 0.5 M K-P$_i$ gradient (pH 7.0). Fractions containing RuBisCO were demonstrated to be isotopically pure, concentrated, and stored in 1 mM Hepes, 1 mM DTT, and 0.1 mM EDTA at 0°C. The [^{35}S]RuBisCO concentration was determined by assaying activity versus a known concentration of active RuBisCO; the specific activity was 5800 Ci/mol.
54. Initial complex formation was achieved by adding ATP (final concentration of 100 μM) to 180 nM GroEL$_{14}$ with or without 700 nM GroES$_{14}$ in folding buffer [100 mM Na Hepes, 5.0 mM $Mg(CH_3CO_2)_2$, 1.0 mM DTT, 0.50 mM KCH_3CO_2, 0.10 mM EDTA, and 0.010% Tween-20]. After allowing 1 min for formation of the asymmetric complex (when GroES was present), we rapidly added four aliquots (5 μl each) of ~400 nM [^{35}S]RuBisCO (acid-denatured) (a total of 66.7 nM RuBisCO added), and the quaternary complex was isolated by gel filtration in folding buffer (Bio-Sil Sec 400-5; 7.8 mm by 300 mm; Bio-Rad). We isolated ≥25% of the starting disintegrations per minute as a stable complex with GroEL (eluting at ~18 nM GroEL or asymmetric complex).
55. We achieved simultaneous addition of acid-denatured RuBisCO and other components by balancing the added components on the side of the tube until acid-denatured RuBisCO could be rapidly added, then vortexing thoroughly.
56. Because of the instability of RuBisCO-I over time, especially with aggregation constantly reducing the concentration of free RuBisCO-I (Fig. 3), complete isotopic equilibrium may occur at a relatively higher concentration of RuBisCO-I retained.
57. We thank T. R. Webb for technical assistance in the purification of the proteins used in these studies.

5 April 1994; accepted 6 July 1994

Integration and Germ-Line Transmission of a Pseudotyped Retroviral Vector in Zebrafish

Shuo Lin, Nicholas Gaiano, Patricia Culp, Jane C. Burns, Theodore Friedmann, Jiing-Kuan Yee,* Nancy Hopkins†

The zebrafish is rapidly becoming a popular model system for the study of vertebrate development because it is ideal for both embryological studies and genetic analysis. To determine if a retroviral vector pseudotyped with the envelope glycoprotein of the vesicular stomatitis virus could infect zebrafish embryos, and in particular, the cells destined to become the germ line, a pseudotyped virus was injected into blastula-stage zebrafish embryos. Fifty-one embryos were allowed to develop and eight transmitted proviral DNA to their progeny. Founders were mosaic, but as expected, transgenic F_1's transmitted proviral DNA in a Mendelian fashion to the F_2 progeny. Transgenic F_1 fish inherited a single integrated provirus, and a single founder could transmit more than one viral integration to its progeny. These results demonstrate that this pantropic pseudotyped vector, originally developed for human gene therapy, will make the use of retroviral vectors in zebrafish possible.

That retroviruses could be used to deliver foreign DNA into the genome of an animal was first demonstrated by infecting preimplantation stage mouse embryos with the Moloney murine leukemia virus (MoMLV) and obtaining germ-line transmission of an integrated provirus (*1*). Subsequently, the ability of retroviruses to integrate exogenous DNA into the genome of infected cells has been exploited for gene therapy (*2*), for cell lineage studies (*3*), and for studies of insertional mutagenesis (*4, 5*). In addition, the use of retroviral gene traps in conjunction with mouse embryonic stem cells has proven quite effective in the search for, and mutagenesis of, genes expressed during mouse development (*5*).

In recent years the zebrafish, *Danio rerio*, has become a popular model system for vertebrate developmental studies because it offers the opportunity to combine classical genetic analysis, including large-scale mutagenesis, with an easily accessible and manipulatable embryo. Genetic studies of the zebrafish benefit from the 2- to 3-month generation time, the ability of females to routinely lay hundreds of eggs, and the small size of the adults, whereas embryological studies benefit from the large, transparent embryos, detailed fate maps, and the fact that single identified cells can be studied in living embryos (*6*). In the past, the application of retroviral vector technology to the zebrafish system was not feasible because of the limited host range of the standard vectors. However, a recent report has demonstrated that a pseudotyped retroviral vector, which can be concentrated to very high titers, can infect cultured fish cells, including those derived from zebrafish embryos (*7*). This virus contains an MoMLV-based genome surrounded by an envelope containing the glycoprotein (G protein) of the vesicular stomatitis virus (VSV), completely replacing the retroviral *env* glycoprotein. As a result of the presence of the VSV G protein, this pseudotyped virus has the broad host range characteristic of VSV, and on entry into a permissive cell will integrate retroviral sequences into the host genome.

The ability of the MoMLV(VSV) pseudotyped virus to infect cultured fish cell lines suggested that it might be possible to infect zebrafish embryos and to obtain germ-line transmission of integrated proviral DNA. However, because zebrafish embryos develop very rapidly and at 28°C whereas murine retroviruses generally require over 6 hours at 37°C to synthesize and integrate proviral DNA (*8*), it was unclear whether or not germ-line transmission could be obtained efficiently or at all in zebrafish. In these studies we describe the high-frequency infection of the zebrafish germ line with this pseudotyped virus and discuss its potential use in the study of zebrafish development.

A concentrated stock of the pseudotyped virus LZRNL(G) (Fig. 1) was generated essentially as described (*9*). This virus was titered on cultured zebrafish cells by infection of an established zebrafish cell line, PAC2 (*10*), and selection for clones in media containing G418 (*11*). LZRNL contains the neomycin phosphotransferase gene (*neo*) and thus can confer G418^r resistance to infected cells. Control mouse 3T3 cells were infected under the same conditions. The titer of the virus was 6.7×10^6 colony-forming units (CFU) per milliliter on zebrafish PAC2 cells, and 2.5×10^7 CFU/ml on mouse 3T3 cells.

To generate transgenic zebrafish, we injected LZRNL(G) virus into the blastoderm, among the cells of blastula-stage embryos, at approximately the 2000- to 4000-cell stage (*12*). On the basis of the virus titer on PAC2 cells and the volume injected, we estimate that 50 to 100 infectious units were injected into each embryo.

S. Lin, N. Gaiano, P. Culp, N. Hopkins, Center for Cancer Research and Department of Biology, Massachusetts Institute of Technology, Cambridge, MA 02139, USA.
J. C. Burns, T. Friedmann, J.-K. Yee, Department of Pediatrics and Center for Molecular Genetics, University of California at San Diego School of Medicine, La Jolla, CA 92093, USA.
*Present address: Department of Pediatrics, City of Hope, Duarte, CA 91010–3000, USA.
†To whom correspondence should be addressed.